Realignment of a smectic-*A* phase with applied electric field

Alison Findon,[1] Helen Gleeson,[1] and John Lydon[2]
[1]*Department of Physics and Astronomy, Manchester University, Manchester M13 9PL, United Kingdom*
[2]*Department of Biochemistry, Leeds University, Leeds LS2, United Kingdom*
(Received 12 April 2000)

The realignment of a smectic-*A* phase contained in a conventional display device (with a mesophase layer ~10 μm thick) in response to an applied electric field has been studied using polarizing microscopy and x-ray diffraction. The initial state of the mesophase was a highly aligned focal conic texture. The applied field created a striated texture with parallel (but not equally spaced) disclination lines which appeared to be created in pairs. The lines seem to grow from disclination ''eyes'' in the original texture, linking them first in pairs, and then in long chains, as the field is increased. We suggest that the center of each pair of striations corresponds to a disclination wall and that the texture consists of a parallel array of smectic layers arranged in concentric flattened half-cylinders. Previous electro-optic studies of cells of this type have described the striated, field-on texture but appear to have overlooked the role of the defects in the original texture as growth points for the striations. However, there are structural similarities with two related studies where the field-induced disturbance of the mesophase starts with the production of toroidal focal conics—similar to those we propose.

PACS number(s): 61.30.Gd, 61.30.Jf

INTRODUCTION

When the first generation of liquid-crystal (LC) electro-optic display devices was being developed and manufactured during the 1960s and 1970s, the current opinion was that the nematic phase offered the most valuable electro-optic properties. The twisted nematic device was supreme and it was thought that the higher viscosity of the smectic phases would make them unsuitable for any significant liquid-crystal display (LCD) use. Only in rare, specialist devices, particularly where slow speed of response was no detriment, was a role seen for them. The high resolution smectic display constructed for the projection of ordnance survey maps was such a case [1]. In that device, the image was written on the display by a laser and the electro-optic response was involved only in the initial texture alignment and in any erasure of errors.

The picture changed drastically when it was appreciated that the tilted, chiral smectic phases can have rapid electro-optic responses resulting from reorientation of molecules within an existing layer structure (rather than the reorientation of the layers). The main thrust of LC device research accordingly changed direction in the 1980s and 1990s to focus on the ferroelectric properties of such phases, and in particular the Sm-C^* phase. The pattern of molecular alignment in ferroelectric devices is complex and has been the subject of much investigation. The major source of the complexity is the chevron structure spontaneously adopted by the mesophase when the device is filled. In a program of study intended to investigate the origins of this texture and its associated electro-optic properties, we have constructed and examined display cells containing nonchiral smectic-*A* and smectic-*C* phases. Smectic-*C* phases almost always form chevron structures because of their temperature-dependent tilt angle [2], though there have been a few references to high tilt systems exhibiting a direct Sm-*C* to isotropic phase transition in which there is no chevron structure [3]. Smectic-*A* phases sometimes form chevrons [4–9] and sometimes adopt a nonchevron texture. This paper describes the electro-optical properties of a thin Sm-*A* device without a chevron structure. Its optical texture when filled, the change in appearance of the texture under applied field, and the alignment as studied by x-ray diffraction are reported.

The nature of the electric-field-induced transition from a planar to homeotropic texture in Sm-*A* devices is of particular interest, bearing in mind that the initial states are never completely planar, nor do the final states appear completely homeotropic. The term ''Fréedericks'' transition is used to describe a liquid-crystal realignment caused by applied external fields (either electric or magnetic) which involves a deformation of the director field with no change in the local short-range mesophase structure. This is a texture change rather than a phase change. A classic Fréedericks transition is depicted in Fig. 1(a), where a nematic device with a mesophase of optically positive dielectric susceptibility, between substrates treated to give a homogeneous alignment, is shown in the field ''off'' state and in the ''on'' state, subjected to an electric field above threshold. The applied field is not sufficient to override the surface alignment forces but it does distort the central region of the sample. Although the magnitude of the distortion of the director field depends on the values of k_{11} and k_{33} (splay and bend elastic constants, respectively), the threshold voltage at which the effect begins to appear is dependent only on the value of k_{11}.

It is reasonable to expect that the realignment of a smectic phase under similar circumstances would involve an analogous Fréedericks type of transition, Fig. 1(b). However, this does not appear to be the case. There seem to be at least two complicating factors. The first arises from the difference between the elastic constants in the nematic and smectic phases. The bend elastic constant k_{33} diverges strongly on approaching the Sm-*A* phase from the nematic phase [10] and the bend deformation is severely hindered in the layered Sm-*A* phase. Further, the layer compression modulus in

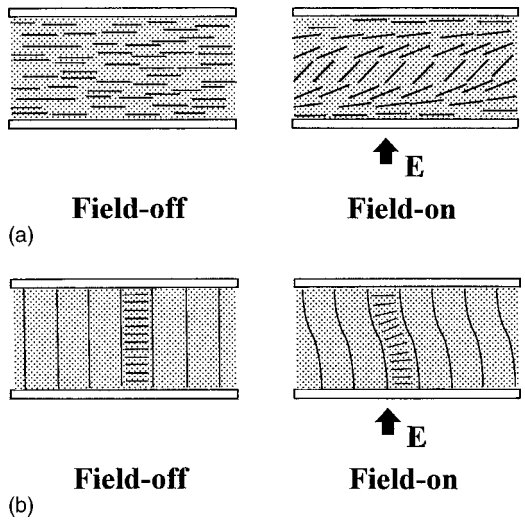

FIG. 1. (a) Fréedericks transition in a nematic device of positive $\Delta\varepsilon$. (b) The corresponding Fréedericks effect for a smectic phase [i.e., the sketch shown in (a) with smectic layers drawn at right angles to the nematic director]. If the amplitude of the displacement is calculated from known values of the elastic constants of the mesophase, it appears that the magnitude is extremely small. An effect of this type will not be observable and it has therefore been termed a ''ghost'' transition [11].

smectic liquid crystals, *B*, plays a role in making the Freedericks transition unobservable. In a bookshelf geometry, amplitude of the distortion of the layer normal from the equilibrium position, θ_m, is given by [11]

$$\theta_m^2 \leqslant \frac{2\varepsilon_0 \Delta\varepsilon E^2}{B} = 2\left(\frac{\pi\lambda}{d}\right)^2,$$

where $\Delta\varepsilon$ is the dielectric anisotropy of the material, E is the applied electric field, d is the device thickness, and λ is the smectic characteristic length ($\lambda = k_{11}/B$). λ is typically of the order of a few layer thicknesses, so θ_m is very small, even in the favorable case of the allowed splay distortion, making the Fréedericks transition a ''ghost'' effect in the terminology of Rapini [11]. The second factor (which is the major concern of this paper) is that the field-on state is not a uniform texture and consists of a parallel set of defect lines. Clearly any discussion of the electrical response must be given in terms of the structure and the pattern of growth of these defects.

There have been a number of previous studies of electric field effects in Sm-*A* devices carried out over the last ten years [12–14]. In all cases, the researchers all found that a straightforward Freedericks transition does not occur. The high field state is a striated texture, dense with defects. It is not immediately obvious how the smectic layers are aligned in this striated state and alternative models have been proposed. Rout and Choudray [12] have proposed a model involving an array of edge dislocations, as sketched in Fig. 2(a). In contrast, Goscianski *et al.* [13], developing a suggestion of Parodi [14], have proposed the grain-boundary model shown in Fig. 2(b).

This paper concerns the way in which the striations grow out of the focal conic ''eyes'' in the defect texture on application of an electric field to a relatively thin, planar aligned,

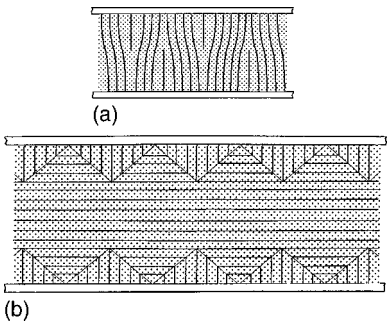

FIG. 2. Models proposed for the striated texture that occurs in smectic-*A* devices following the application of a high field. (a) Rout and Choudray [12] and (b) Goscianski *et al.* [13] and Parodi [14]. Note the way in which the planar surface anchoring is retained but the layers in the center of the sample are completely realigned. In our opinion these are two factors likely to be present in the texture but we consider that a smectic-*A* phase is not likely to form hard-edged grain boundaries of this type.

positive dielectric anisotropy, smectic-*A* sample. Analogous investigations of related systems have been reported by Hareng *et al.* [15] and Li and Lavrentovich [16]. The former of these studies concerns a device similar to ours but appreciably thicker (where there is an apparently different pattern of behavior because disclinations arise within the bulk of the working mesophase). The latter study is, in a sense, the double negative of the system we have examined and concerns a material of negative dielectric anisotropy, initially aligned homeotropically.

EXPERIMENTAL

The experimental techniques employed to study the electric field effects on the smectic-*A* liquid-crystal devices include optical microscopy, electro-optic measurements, and moderately small-angle x-ray scattering. The materials used were denoted TCN9 and TCN10 and their chemical structures and phase sequences are shown in Fig. 3. For all of the measurements, the material was held in a conventional device configuration in planar-aligned glass cells with transparent indium-tin oxide electrodes which allow the application of an electric field to the sample. The device thickness was approximately 6 μm (i.e., relatively thin). Where the device was to be examined via small-angle x-ray scattering, thin glass (approximately 120 μm thick) was used. The geometry of the device used in this investigation and the structures of the idealized bookshelf and homeotropic alignments for the field on and field off cases are shown schematically in Fig. 4.

TCN9	**heating**	$\mathbf{K} \underset{70\,^\circ\mathrm{C}}{\rightarrow} \mathbf{S_A} \underset{96\,^\circ\mathrm{C}}{\rightarrow} \mathbf{I}$
	cooling	$\mathbf{K} \underset{60.3\,^\circ\mathrm{C}}{\leftarrow} \mathbf{S_C} \underset{60.4\,^\circ\mathrm{C}}{\leftarrow} \mathbf{S_A} \underset{95\,^\circ\mathrm{C}}{\leftarrow} \mathbf{I}$
TCN10	**heating**	$\mathbf{K} \underset{65\,^\circ\mathrm{C}}{\rightarrow} \mathbf{S_A} \underset{101\,^\circ\mathrm{C}}{\rightarrow} \mathbf{I}$
	cooling	$\mathbf{K} \underset{62.0\,^\circ\mathrm{C}}{\leftarrow} \mathbf{S_C} \underset{62.1\,^\circ\mathrm{C}}{\leftarrow} \mathbf{S_A} \underset{100\,^\circ\mathrm{C}}{\leftarrow}$

FIG. 3. Molecular structures and mesophase ranges for TCN9 and TCN10. The transition temperatures are in degrees Centigrade.

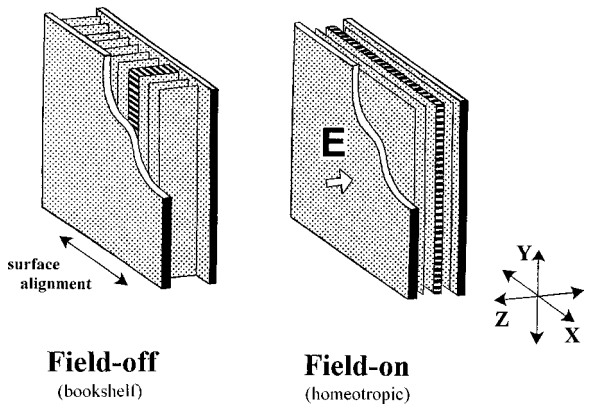

FIG. 4. Geometry of the cell used in this investigation and the structures of the idealized ''bookshelf'' and homeotropic alignments for the field-off and the field-on states. The bookshelf geometry is totally dominated by initial epitaxial alignment at the substrate surfaces and the homeotropic state results from the total realignment of the molecules by the applied field. In practice, neither of these states is achieved: the initial state is a highly aligned focal conic fan texture as shown in 9(c) with occasional eye defects shown in Figs. 9(d) and 9(e). The final state is the striated array of defects sketched in Fig. 10.

The liquid-crystal samples were held in temperature-controled ovens which stabilized the temperature with an accuracy of $\pm 0.05\,^{\circ}\mathrm{C}$ during the experiments. The polarizing microscopy was carried out using an Olympus BH2 polarizing microscope. Electro-optic measurements were performed on a optical rail equipped with a laser diode light source and photodiode detector. The voltages applied to the samples were produced using a signal generator and a wide band amplifier constructed in house. Small-angle x-ray experiments were undertaken at the Synchrotron Radiation Source, Daresbury Laboratory, UK on station 2.1, in a configuration described in detail previously [17].

RESULTS

Description of the optical texture changes with applied field

The initial sample, with no applied field, showed the typical focal conic domain structure shown in Fig. 5. The sample was held at a temperature of $67.9\,^{\circ}\mathrm{C}$ and an alternating voltage at 1 kHz was applied across the plates of the device. Note the way in which the domains are elongated in the *X* direction and the scattering of very obvious bright Maltese cross ''eyes'' showing the positions of the occasional focal conic domains aligned with their axes along the *Z* direction.

There was little discernible change in the texture until a voltage of about 57 V rms (at 1 kHz) was applied. (Note that this is a significantly high voltage as compared with that required to have to have a noticeable effect on the optical texture of an S_C or S_{C*} phase.) Above this threshold field, defect lines appeared. These were parallel to the *Y* direction and they appeared to grow in pairs from the Maltese cross eyes of the focal conic structure, first linking adjacent eyes. As the voltage was raised further, the defect lines extended throughout the mesophase and became more numerous. Finally at an applied field of about 110 V rms, the focal conic eyes had more or less disappeared and the whole sample was striated from top to bottom. On removing the applied field, some of the lines retreated and a few disappeared altogether—but the overall striated appearance was retained

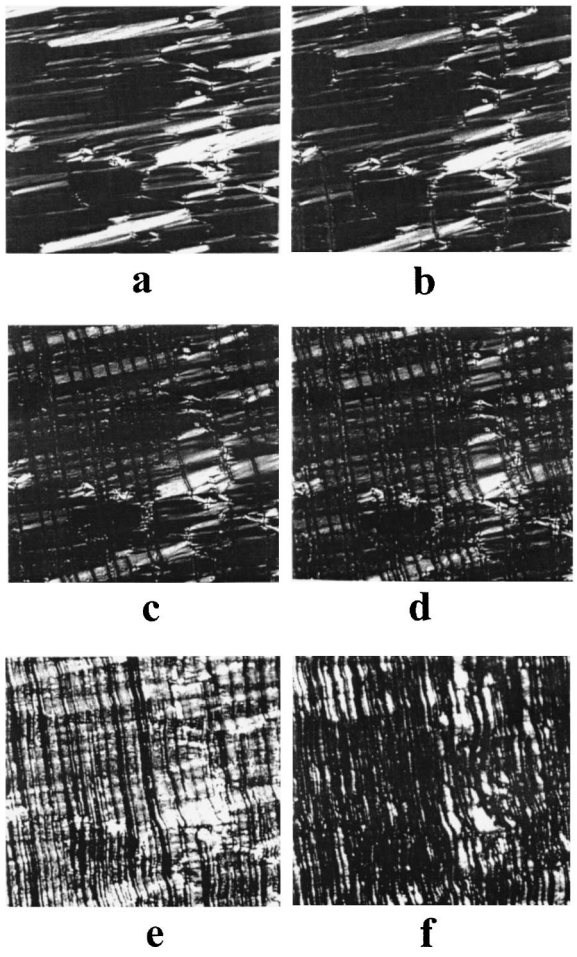

FIG. 5. The change in optical texture with applied field. These optical micrographs show a $500\times500\,\mu\mathrm{m}^2$ region of the cell as seen between crossed polars (parallel to the *X* and *Y* axes as defined in Fig. 4). The conditions under which each frame was taken correspond to the lettered positions on the electro-optic response curve shown in Fig. 7.

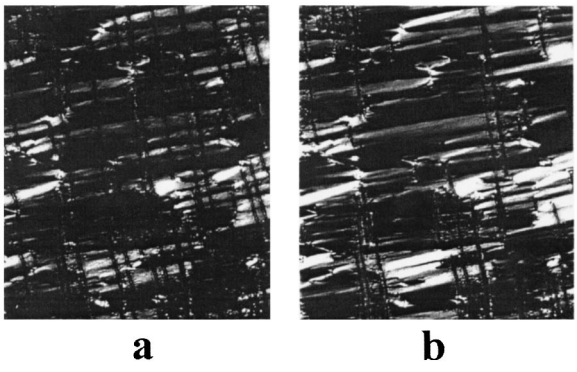

FIG. 6. (a) The field-on texture for an applied voltage of 62 V and (b) its retention when the applied voltage is removed. These micrographs were taken under crossed polars as for Fig. 5. The texture change occurred almost immediately and the reduced number of defect lines apparent in (b) appeared to be stable.

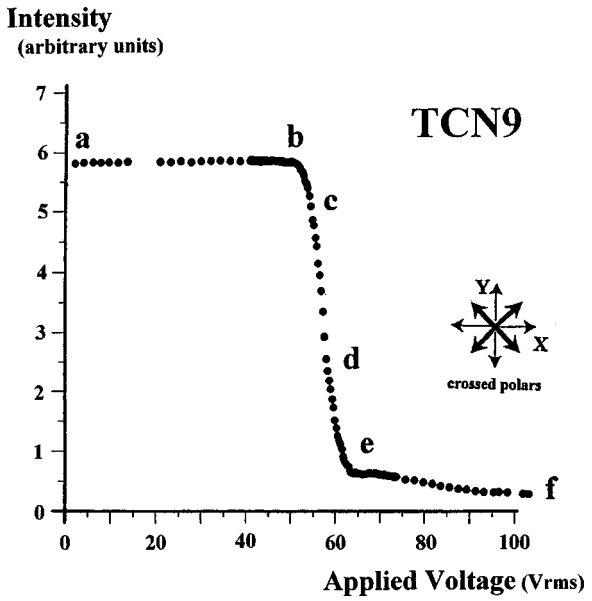

FIG. 7. The electro-optic response of a 6.53-μm-thick sample of TCN9 at a temperature of 67.9 °C. This graph shows the change of transmitted intensity as the applied field is increased. Note that here the sample is viewed between crossed polars lying at 45° to the *X* and *Y* directions—in contrast to the optical micrographs shown in Figs. 5 and 6 where the crossed polars are parallel to *X* and *Y*. The letters $a-f$ indicate the conditions under which the optical micrographs shown in Figs. 5 and 6 were recorded.

for at least a period of several hours. Figure 6 shows the appearance of the device on removal of an applied voltage of 62 V.

Electro-optic response and x-ray studies

The electro-optic response of the 6.5-μm-thick device containing TCN9 is shown in Fig. 7. Note that here the sample is viewed between crossed polarizers with the optic axis in the field off state at 45° to the polarizer directions. This is in contrast to the optical micrographs shown in Figs. 5 and 6, where the crossed polarizers are parallel to *X* and *Y*. There is an obvious switching threshold at position **b**. and there is essentially no change in the transmitted light intensity before that threshold is reached.

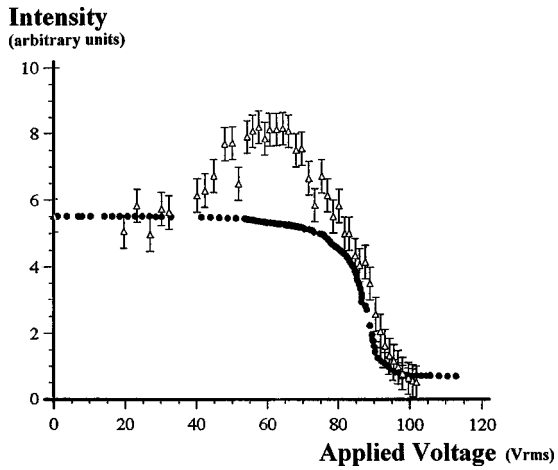

FIG. 8. The change in the intensity of the x-ray peak with voltage for an 8-μm-thick sample of TCN10 at 68.8 °C, held approximately normal to the incident x-ray beam (open triangles). In this orientation, the sample is not quite in the Bragg condition for a perfect bookshelf alignment and the intensity at 0 V is the shoulder of the Bragg peak. As the applied voltage increases and the director field becomes realigned, some of the smectic layers move through the Bragg condition giving an increase in intensity before moving completely out of it. For comparison, the electro-optic data for this sample have been added and are shown as closed circles. The sample temperature was 70 °C.

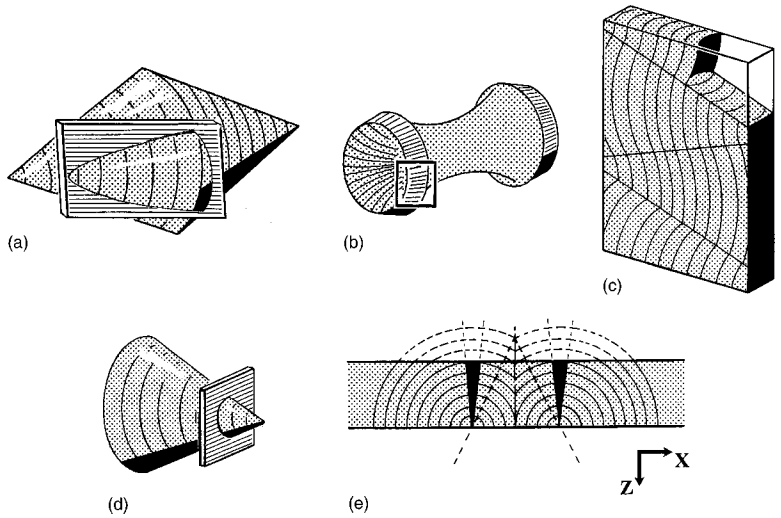

FIG. 9. The rationale for the initial aligned focal conic texture. (a) and (b) show how an oblique plane cutting through a focal conic unit intersects layers of molecules with a common parallel alignment. Presumably this explains why the mesophase adopts the aligned focal-conic texture since it allows the maximum number of molecules to follow the epitaxial alignment whilst still retaining the focal-conic structure. Note that in this experiment, the cell is much thinner than the diameter of the focal-conic units and the sketch shown in (c) gives a reasonably realistic impression of the curved arrays of saddle-shaped layers in the observed fan texture. In contrast, the eyes occur where the central axis of a focal-conic unit lies more or less normal to the cell surfaces, as sketched in (d). We picture the arrangement of layers around these eyes to extend from the focal-conic cones to meet the cell surface, giving half Dupin cyclide structures as sketched in (e). The solid black wedges in this sketch indicate regions where the layer alignment is strictly homeotropic.

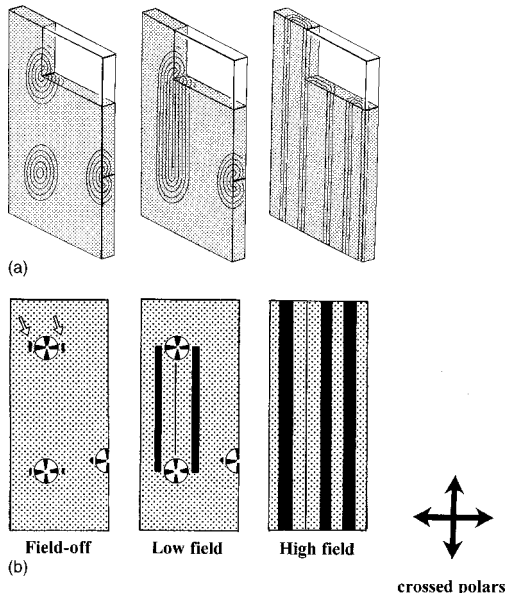

FIG. 10. (a) The director field patterns for zero-field, low-field, and high-field states of the cell. Note the way in which the small homeotropic regions present in the initial field-off state extend under the influence of the applied field. (b) Stylized sketch showing the optical textures of the cell in the field-off, low-field, and high-field states. The solid black areas indicate regions where there is a homeotropic alignment of the smectic layers and which will therefore appear black between crossed polars.

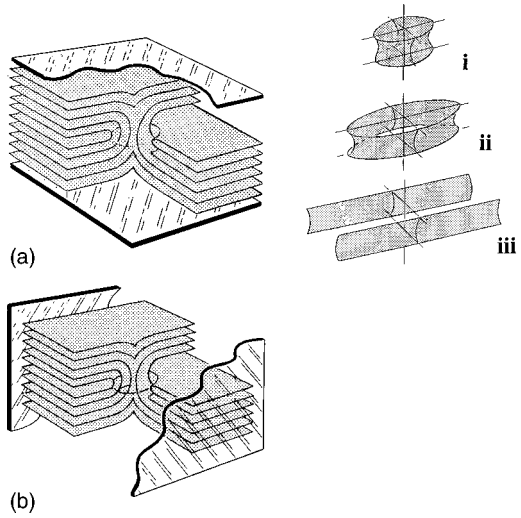

FIG. 11. The response of THICK smectic-*A* samples to applied electric fields described by previous investigators. (a) The postulated toroidal disclination within the bulk of the mesophase for a device in an initial homeotropic alignment (redrawn from [16]). Figures (i), (ii), and (iii) represent the progressive distortion of the ''eyelet''-shaped smectic layers for a negative $\Delta\varepsilon$ sample as the applied field is increased. (b) The analogous distortion postulated by Hareng *et al.* [15] for a device in an initially planar, positive $\Delta\varepsilon$ sample. Although working with systems of different alignment and or sign of anisotropy, our response is remarkably consistent with these though the defects are anchored on the surface, resulting in the patterns indicated in Fig. 10, which corresponds to one-half of (b).

The smectic-layer structure within the sample, studied by small-angle x-ray scattering, was initially found to be in an almost ideal bookshelf geometry. This is in contrast with some x-ray studies of Sm-*A* devices where small-angle chevron structures formed in the device [9]. The device considered here was held in the Bragg condition (almost normal incidence) and the intensity of the Bragg peak monitored as a function of applied voltage, Fig. 8. The electro-optic response is also shown on Fig. 8 for comparison. It can be seen that there is a small change in the intensity of the Bragg peak prior to the optical threshold. This indicates that there is some small reorganization or motion of the layers from the point when the field is first applied. At first sight this diagram appears to imply a rather large effect, but it should be remembered that any small motion of the layers out of the Bragg condition gives rise to a large change in the diffracted intensity. Gross reorganization of the layers appears to coincide with the optical threshold. It is worth commenting briefly on the difference in threshold voltages between Figs. 7 and 8. The threshold voltage varies as the square root of the cell thickness in these systems [18], but also depends on the liquid-crystal material and the temperature. Indeed the threshold fields associated with the two data sets are not the same and the detailed dependence of threshold voltage on cell thickness and other parameters, including surface anchoring energy, will be discussed in a future publication.

DISCUSSION: EXPLANATION OF THE TEXTURE CHANGES WITH APPLIED FIELD

The initial state at zero applied field is a partially aligned focal-conic structure. The elongation of the focal conic units in the *Y* direction arises presumably because this allows the maximum number of mesophase molecules in contact with the surface, to be aligned parallel to the rubbing direction, as shown in Figs. 9(a) and 9(b). Figure 9(c) is a more realistic impression of the layers taking into account the cell thickness. Figures 9(d) and 9(e) depict the arrangement in and around the central axes of the focal conic units. These figures appear to offer a satisfactory explanation for the observed pairing of the striations on application of a field, as follows.

The applied field attempts to realign the mesophase into a homeotropic state where the molecules lie perpendicular to the cell faces (i.e., parallel to the *Z* direction). If we had been dealing with a tilted smectic phase (an S_C or S_{C*}), there would have been some room for maneuver—with the molecules being able to rotate around their alignment cones whilst keeping the layer structure unchanged. However, there is no possibility of such a thing in this case—and for the molecules to realign, the layer structure has to change also (hence the high value of the threshold field and the relatively small motion implied by the small change in Bragg intensity up to the optical threshold point).

The simultaneous realignment of molecules and layers appears to start at the points of weakness in the structure—the focal conic eyes. We suggest that the realignment process for a planar-aligned sample of a dielectrically positive Sm-*A* material follows the stages sketched in Figs. 10(a). Figure 10(b) is a schematic of the optical texture corresponding to the three states shown in Fig. 10(a). The solid black areas indicate field-induced homeotropic alignment which would be black between crossed polarizers.

It is worth commenting on the most obvious difference

between the situation described by Li and Lavrentovich and that reported here. The symmetry of the situation here causes the striations to occur in a well-defined direction (parallel to the *Y* axis), whereas the field-induced texture in the homeotropic, negative $\Delta\varepsilon$ case has no preferred elongation direction within the *X*-*Z* plane in the field-on state and the pattern of growth of the planar regions is perhaps best described as ''wormlike'' rather than striated. The structure of the layers in the toroid in the homeotropic sample examined by Li and Lavrentovich can be described as initially circular ''eyelets'' as shown in Fig. 11. Any departure from this highly symmetrical situation would produce an elliptically shaped toroid as shown in Fig. 11. It can be seen that there is a considerable energetic difference between the energy of the layers intersecting the major and minor axes of the ellipse, with a greater proportion of the material at the major axis in an energetically favorable state with respect to the applied field. This explains the form of wormlike growth extending from any initial irregularities in the pattern. Although there are minor differences in the pattern of growth and the fact that in our situation the defects are present in the initial field-off state, the correspondence between the two cases is striking. The model that we have proposed here based on curvature and interpretation of the optical texture changes appears to be more compatible with the known properties of Sm-*A* phases than the alternative models previously proposed for this deformation shown in Figs. 2(a) and 2(b). The basic distinction between previous investigations [15,16] and our studies is that for thicker samples the toroidal dislocations form within the bulk of the sample, whereas for thinner cells they appear to be anchored on the surfaces. The model suggested here is developed further by investigating the field effects as a function of molecular structure and device thickness in a future publication.

CONCLUDING COMMENT

Our observations indicate that the striations in the high-field texture grow from the focal conic eyes in the original field-off texture—and we postulate that it is actually the small regions of homeotropic alignment lying beside the eyes where the ''seeding'' starts. A mechanism of this type would explain the poor level of conformity between the results obtained by different groups of workers [13,19] since it is unlikely that the initial states of the cells were identical. It would be interesting to examine the effects of controlled seeding of the substrate surfaces.

Extending the idea further, we suggest that this effect may be utilized to give a novel type of electro-optical device. If the substrate surfaces are treated to give a regular geometric array of focal-conic eyes then the field-on state would be an equally spaced set of disclination lines, i.e., a diffraction grating that can be switched on or off and which is effectively transparent in the off state. Switchable diffraction gratings have been constructed using more conventional LCD technology [20] but there may be advantages (in robustness possibly) in using a smectic phase.

ACKNOWLEDGMENTS

A.F. gratefully acknowledges support from the Engineering and Physical Science Research Council and the Defense Evaluation Research Agency.

[1] F. J. Kahn, Appl. Phys. Lett. **22**, 111 (1973).
[2] *Ferroelectric Liquid Crystals*, edited by J. W. Goodby *et al.* (Gordon and Breach, New York, 1991).
[3] P. Lehmann, W. K. Robinson, and H. J. Coles, Mol. Cryst. Liq. Cryst. Sci. Technol., Sect. A **238**, 221 (1999).
[4] J. Stamatoff, P. E. Cladis, D. Guillon, M. C. Cross, T. Bilash, and P. Finn, Phys. Rev. Lett. **44**, 1509 (1980).
[5] Y. Takanishi, Y. Ouchi, H. Takezoe, and A. Fukuda, Jpn. J. Appl. Phys., Part 1 **28**, L-487 (1989).
[6] Y. Ouchi, Y. Takanishi, H. Takezoe, and A. Fukuda, Jpn. J. Appl. Phys., Part 1 **28**, 2547 (1989).
[7] L. Limat and J. Prost, Liq. Cryst. **13**, 101 (1993).
[8] A. S. Morse and H. F. Gleeson, Liq. Cryst. **23**(4), 531 (1997).
[9] G. Srajer, R. Pindak, and J. Patel, Phys. Rev. A **43**, 5744 (1991).
[10] P. J. R. Birtwistle, Ph.D. thesis, Manchester University, Manchester UK, 1995 (unpublished); H. F. Gleeson, *The Liquid Crystal Handbook*, edited by D. Demus Vill *et al.* (VCH-Wiley, Weinheim, 1998), Chap. 8.
[11] A. Rapini, J. Phys. (Paris) **33**, 237 (1972).
[12] D. K. Rout and R. N. P. Choudray, Mol. Cryst. Liq. Cryst. **166**, 75 (1989).
[13] M. Goscianski, L. Leger, and A. Mircea-Roussel, J. Phys. (France) Lett. **36**, L313 (1975).
[14] O. Parodi, Solid State Commun. **11**, 1503 (1972).
[15] M. Hareng, S. Le Berre, and L. Thirant, Appl. Phys. Lett. **25**, 683 (1981).
[16] Z. Li and O. D. Lavrentovich, Phys. Rev. Lett. **73**, 280 (1994).
[17] H. F. Gleeson, C. Carboni, and A. Morse, Rev. Sci. Instrum. **66**, 3563 (1995).
[18] A. Findon, Ph.D. thesis, Manchester University, Manchester, UK, 1995 (unpublished).
[19] G. Pelzl, H. J. Deutscher, and D. Demus, Cryst. Res. Technol. **16**, 603 (1981).
[20] L. J. Friedman *et al.*, Appl. Opt. **35**, 6236 (1996).